polymer

Structural and kinetic transitions in P(VDF–TrFE)/PMMA blends

L.O. Faria[a],*, R.L. Moreira[b]

[a]*Centro de Desenvolvimento da Tecnologia Nuclear, R. Mário Werneck s/n, C.P. 941, 10123-270, Belo Horizonte, MG, Brazil*
[b]*Depto. de Física, ICEX, UFMG, C.P. 702, 30213-970, Belo Horizonte, MG, Brazil*

Abstract

The miscibility in binary blends of a ferroelectric (vinylidene fluoride–trifluorethylene) copolymer (PVDF–TrFE) and amorphous poly(methyl–methacrylate) (PMMA) has been investigated over the full range of compositions for the copolymer with 50% wt. of trifluorethylene (TrFE). The kinetics of glassy and ferroelectric phase transitions have been studied and we demonstrate the miscibility of the components in the range of 5% to 15% wt. of PMMA. From 20 to 35 wt.% of PMMA, the system can still crystallize and present ferroelectricity, but it becomes strongly thermal history dependent. Above 40% wt., it is completely amorphous. The relationship between optical scattering in the visible range and a room temperature crystallization process has been established. The 15% wt. PMMA sample has been suggested as a very promising host material for non-linear optical and thermoluminescence applications. © 1999 Elsevier Science Ltd. All rights reserved.

Keywords: Vinylidene fluoride–trifluorethylene copolymers; Polymer blends; Ferroelectric phase transition

1. Introduction

Blends of (vinylidene fluoride–trifluorethylene) copolymers [P(VDF–TrFE)] and Poly(methyl–methacrylate) [PMMA] have been proposed as candidates for applications in optical communications technology [1,2]. Due to their excellent Second Harmonic Generation (SHG) and waveguiding properties, they have been used in host–guest systems with nonlinear optical molecules. Enhanced optical transmission efficiency in the visible range can still turn these polymeric blends good candidates as substitute of Poly(vinylidene fluoride) [PVDF] in CaSO4:Mn/PVDF mixtures, for LASER heating thermoluminescense dosimetry applications [3].

Binary blends, with crystalline and amorphous polymers as components, such as PVDF/PMMA, have been extensively studied [4–10]. The morphology and compatibility of such blends have been studied so far, through melting and glass transition temperatures analyses.

P(VDF–TrFE) copolymers present a ferroelectric phase transition for trifluorethylene contents ranging from 18 to 63 mol% [11–15,20]. In this work we shall show how the thermal behavior of the ferroelectric–to–paraelectric phase transitions in blends of P(VDF–TrFE)/PMMA can give unique information about the morphology and miscibility

of polymer blends. We investigate the glassy and the structural transitions and discuss the optical transmission efficiency in terms of the crystallization kinetics.

2. Experimental procedures

Blends of P(VDF–TrFE) with 50% of trifluorethylene (TrFE) and PMMA, with 5, 10, 15, 20, 25, 30, 35, 40, 50 and 70% wt. of PMMA, were prepared by dissolving small quantities (0.03 g/ml), in a solvent formed by *n,n*–dimethylacetamide (DMAc) and 1% Acetic Anhydride at 60°C. After complete dissolution, which is accomplished after 24 h at this temperature, a larger volume of distilled water was added in order to worsen the solvent and to force a fast blend formation. This process produces a gel-like material, which, after drying, still presents amounts of both of DMAc and water, which are completely eliminated after 24 h at 60°C. The samples were then melted at 200°C, pressed (300 bar) and quenched to room temperature. This process allows us to produce good samples, in form of transparent films of c.a. 200 μm, with no degradation, in only two days.

The P(VDF–TrFE$_{50\%}$) was supplied by ATOCHEM and the PMMA was of a commercial type (PLEXIGLASS™).

Thermal analysis was performed by differential scanning calorimetry (DSC) (Mettler TA10-DSC30) at various rates.

---

* Corresponding author. Tel.: + 55-31-499-3363; fax: + 55-31-499-3400.

Fig. 2. Room temperature X-ray diffractograms for P(VDF–TrFE50%)/ PMMA blends with PMMA contents ranging from 0% to 40% wt.
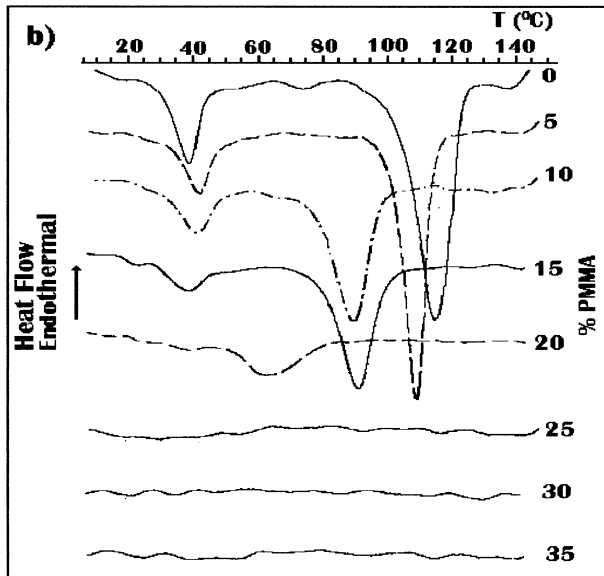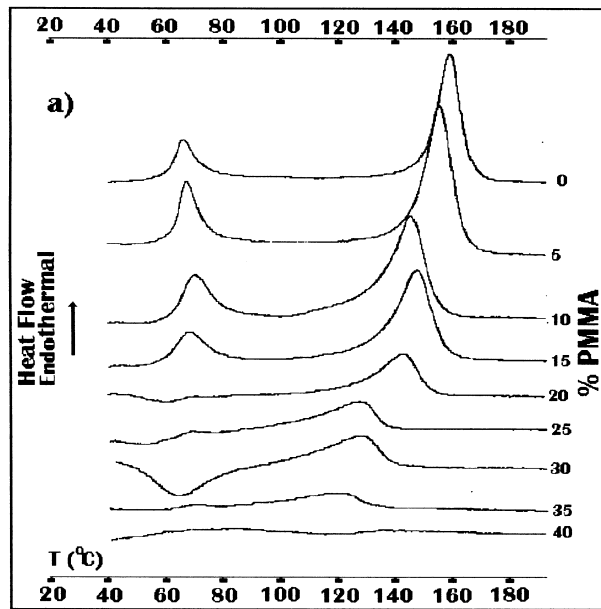
Fig. 1. DSC thermogram for P(VDF–TrFE50%)/PMMA blends with 0, 5,10, 15, 20, 25, 30, 35 and 40 %wt. of PMMA for (a) second heating and (b) subsequent cooling.

Typical sample weights were 10 mg. Optical transmission measurements were taken in a Hitachi U-3501 Spectrophotometer ranging from 190 to 900 nm. Structural studies were made by X-ray diffractometry (Rigaku) with $8°2\theta/\min$ scan rate using CuK_α radiation.

3. Experimental results

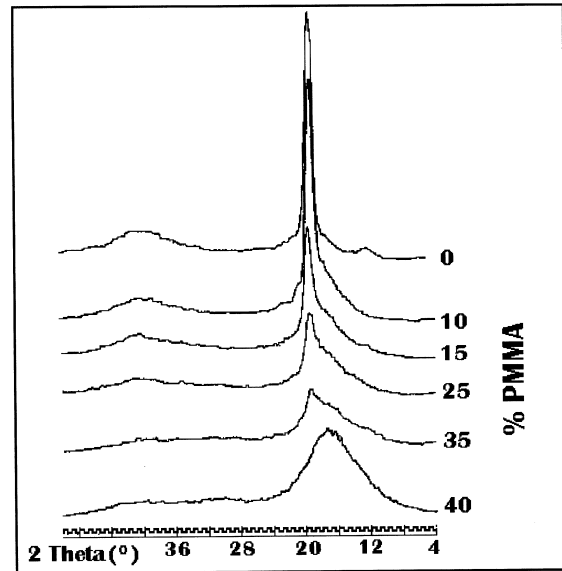The high temperature DSC thermograms for P(VDF–TrFE$_{50\%}$)/ PMMA blends with PMMA contents ranging from 5% to 40%, are shown in Fig. 1, for the second thermal run (two complete cycles were made for each sample, between 20°C and 200°C, at 20°C/min heat/cooling rates). Note that the thermograms of the pure ferroelectric copolymer show two anomalies corresponding to the ferroelectric– paraelectric transition (lower temperature peak) and melting of crystallites (higher temperature one). As seen in Fig. 1(a), the melting temperatures (T_m) of the blends decrease continuously, from 160°C to 120°C, with the increase of the amount of PMMA. In the meanwhile, the Curie transition temperatures (T_c) remain around 66°C and the areas under the melting and phase transition peaks decrease. We can say then that the melting and the phase transition latent heats (H_m and H_{pt}) are decreasing, leading to an increasing amorphization of the blends. Above 35% of PMMA, the blends are totally amorphous (the peaks disappeared).

One can still see in Fig. 1(a) the appearance of an unexpected exothermic peak, instead of the phase transition endothermic one, for the sample with 30% of PMMA.

Fig. 1(b) shows the thermograms for subsequent cooling. Here, the crystallization peak temperatures decrease as the contents of PMMA in the blends increase until 20%. The phase transitions remain at the same temperature until 15% of PMMA.

Comparing Fig. 1, (a) and (b), we can see that the samples with 25, 30 and 35% present melting peaks on heating, but did not show the corresponding crystallization peaks on cooling. It seems to indicate that the system becomes more viscous in these samples, preventing the crystallization during the cooling run. If such hypothesis holds for the sample with 30% of PMMA, which does not show recrystallization on cooling, it will be seen to recrystallize on heating. This could explain the exothermic peak observed with this sample during the thermal heating as a recrystallization in the paraelectric phase.
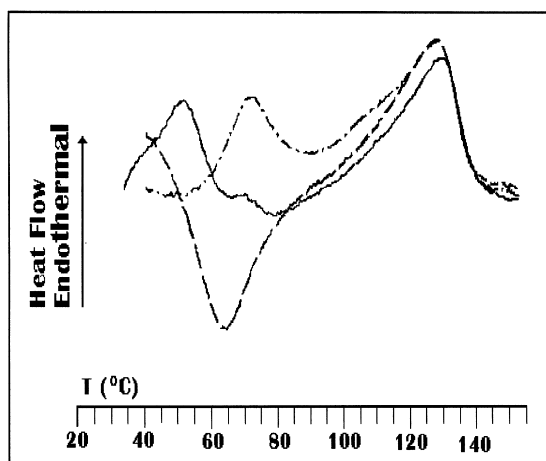
Fig. 3. DSC heating thermograms (20°C/min) for the P(VDF–TrFE50%)/PMMA blend with 30% wt. of PMMA, after storage for one week (–), after subsequent cooling at 20°C/min (– – –) and after annealing at 90°C (---).

In order to verify the structural and crystallinity changes with PMMA contents in the blends indicated by the previous data, we have performed X-ray measurements. Fig. 2 shows the room temperature X-ray diffractograms for the samples of Fig. 1, after long time storage (one week). The crystalline peaks indicate that the samples present the polar β phase of PVDF [14,16] (the main observed peaks are superimposed 200 and 110 around $2\theta = 20°$ and 201 around 41°), which is compatible with the reversible low temperature latent heat observed in Fig. 1, i.e., the samples can undergo the ferroelectric–to–paraelectric phase transition on heating. As the

% wt. of PMMA increases, the positions of these crystalline peaks remain at the same angles, indicating that the crystalline cells of P(VDF–TrFE$_{50\%}$) are not swelling, in the presence of the strange molecular chains of PMMA. The continuous widening of these peaks account for either a decrease of the degree of order in the crystalline cells or a reduction in the crystallite sizes. Since the crystalline cells are not swelling, we believe that the second possibility holds. Using the Scherrer relation [17], the crystallite dimensions along the a and b axes (estimated from the 200 and 110 peaks) decrease from 100 Å (pure copolymer) to 33 Å (35% PMMA). This fact, associated with a probable reduction on their number, may explain the fast system amorphization, which is complete when the amount of PMMA reaches 40%. The point of total amorphization is the same for DSC (Fig. 1) and X-ray diffractograms (Fig. 2).

Let us now return to the thermal investigations of our system. The metastability of the blends for PMMA amounts greater than 20%, indicated by the anomalous crystallization behavior, needs to be examined more carefully. Thus we have investigated the influence of thermal history in the behavior of the sample with 30% of PMMA content (Figs. 3 and 4). Storing this sample at room temperature for more than one week leads to the appearing of an endothermic peak at 55°C (Fig. 3, solid curve), instead of the exothermic one showed in Fig. 1(a). A subsequent heating, after cooling at 20°C/min, provokes the reappearing of the exothermic peak (Fig. 3, dashed curve) seen in Fig. 1(a). Annealing the sample at 90°C for some minutes, i.e., just after the exothermic peak (on heating), leads again to the
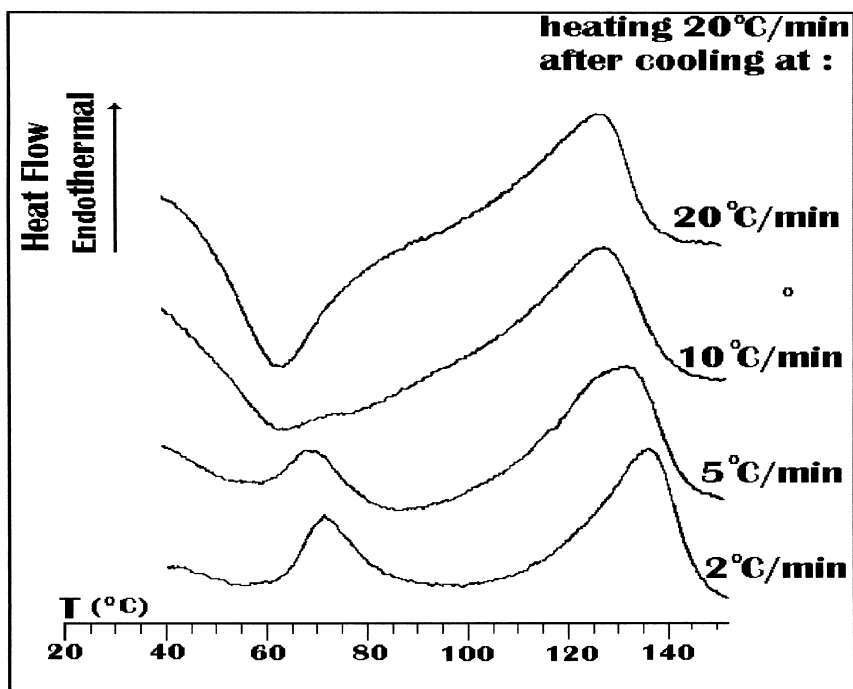

Fig. 4. DSC thermograms for the P(VDF–TrFE50%)/PMMA blend with 30 %wt. of PMMA, heating at 20°C/min, after cooling from the melt at 20, 10, 5 and 2°C/min.
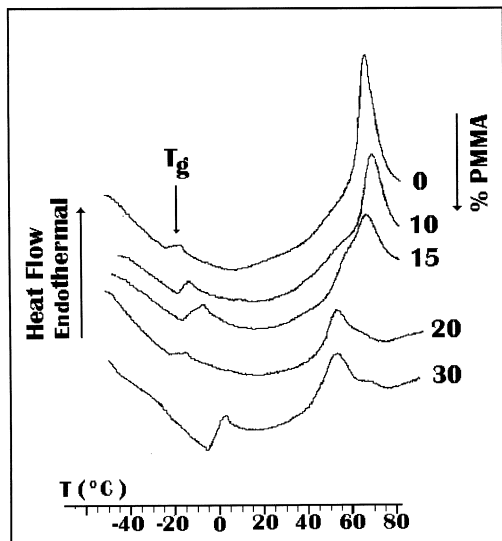
Fig. 5. Low temperature DSC Thermograms for P(VDF–TrFE50%)/PMMA blends, for a first heating at 20°C/min. The samples were previously stored at room temperature for one week, before measuring.

endothermic phase transition peak around 66°C (Fig. 3, dot-dashed curve). In other words, annealing the sample at 90°C, allows the system to crystallize in the paraelectric phase. Cooling it at 20°C/min, leads the system to its ferroelectric phase. In the subsequent heating process, the system will present the Curie transition of its crystalline phase. The melting peaks remained at the same temperature.

Concerning the low temperature peak seen around 55°C, denoting the ferroelectric phase transition, the decreasing of the transition temperature should be a consequence of the room temperature crystallization process, which may produce less perfect crystallites.

In order to study the influence of the cooling rate on the crystallization kinetics, we show in Fig. 4, as an example, the DSC thermograms for the sample with 30% of PMMA content, at the same heating rate of 20°C/min, after different cooling rates from the melt. We can see in these
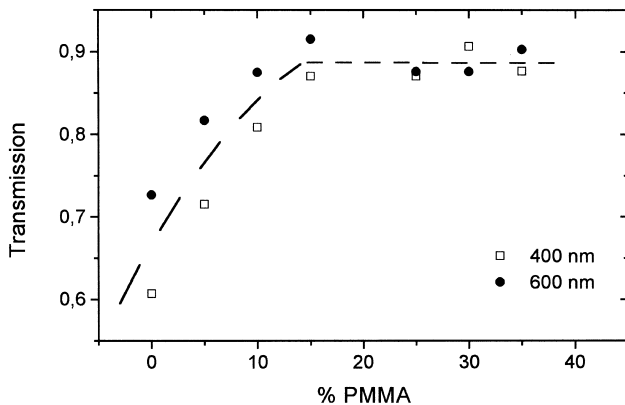
thermograms that, for higher cooling rates (20°C and 10°C/min), the sample has no time to crystallize during the cooling process and then, as has been previously mentioned, it recrystalizes on heating. As the cooling rate decreases, T_m increases and the melting peak become thinner, indicating an increasing of the degree of order. Also, the sample has increasingly more time for crystallization, leading to the gradual appearance of the endothermic phase transition peak.

This kinetic behavior can be explained based on our previous hypothesis that the overall sample viscosity increases with the increase of PMMA contents, probably due to the increasing in the blend glass transition temperature. This effect, associated to the lowering of the crystallization temperatures with PMMA contents [cf. Fig. 1(b)], decreases the chain mobility and prevents crystallization, if the cooling hate is high enough to do so.

We have performed kinetic studies also on the P(VDF–TrFE$_{50\%}$)/PMMA blends with 20, 25 and 35% wt. of PMMA, which show the same behavior of the 30% wt. PMMA sample. Thus, we have looked for quasi-equilibrium samples, storing them at room temperature (RT) for one week, before undertaken the measurements. DSC thermograms were then measured on a first heating, from -60°C to 90°C, on the same group of samples of Fig. 1 and the results are shown in Fig. 5. As it can be seen in this figure, the glass transition temperatures increase with the % wt. of PMMA, until it reaches 15%, indicating that the components are compatible in the amorphous phase. Above 15%, except to the sample with 30%, the T_g observed are the glass transition temperatures of the P(VDF–TrFE$_{50\%}$) copolymer and this fact indicates that the components are not mixed. The value of T_g of PMMA is 95°C and can not be observed in these thermograms. Concerning the sample with 30% wt., we can say that the components have blended as in the samples with 5, 10 and 15%.

Looking at the region of phase transition peaks in this figure, we can clearly observe the low temperature peaks arising as the PMMA content is higher than 15%, indicating the beginning of a room temperature crystallization process. The lowering of the peak transition temperature indicates the presence of less stable (less perfect) recrystallized regions.

Comparing the evolution of the glass and ferroelectric transition peak temperatures, we can state that the P(VDF–TrFE$_{50\%}$)/PMMA can form true blends until 15% of PMMA contents, with the ferroelectric characteristics of the copolymer being preserved. From 20% to 35%, a room temperature crystallization process is present but the blending of the amorphous phase could not be completely achieved, owing to very low chain mobility at the storage temperature.

The kinetic behavior of this system could have important consequences on the optical transmission of the films. Thus, in order to investigate this property correctly, the samples have been previously stored at room temperature for more
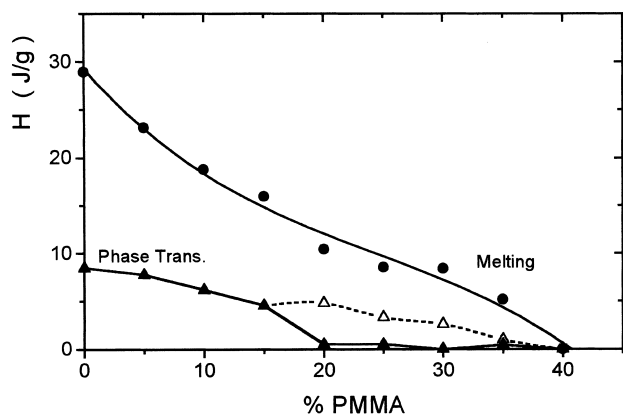

Fig. 6. Variation of the Optical Transmission of P(VDF–TrFE50%)/PMMA blends with the PMMA % wt. in 400 nm (open square) and 600 nm (solid circle).

Fig. 7. Melting and ferroelectric phase transition latent heats upon heating, per gram of sample, of P(VDF–TrFE50%)/PMMA blends, for the data of Fig. 1 (full symbols). The open triangles represent the data after annealing the samples at 90°C.

than one week. The results are presented in Fig. 6. The variation of the optical transmission efficiency with the PMMA contents seems to be related to the room temperature crystallization process. As it is seen in Fig. 6, the optical transmission at the extremities of the visible range (400 and 600 nm) increases in a continuous manner until the PMMA % wt. is 15%. Above this value, the data do not follow a regular curve.

This behavior can be explained by optical scattering in the crystallites [1]. As the PMMA contents increases from 0% to 15%, the crystallite sizes decrease (as seen in X-ray diffractograms of Fig. 2), reducing gradually the losses due to optical scattering. Above this value, as shown by Fig. 5,

room temperature crystallization takes place, producing less perfect crystallites and changing the scattering pattern.

4. Discussion

As the PMMA % wt. increases in P(VDF–TrFE$_{50\%}$)/PMMA blends, the system becomes less crystalline, turning itself completely amorphous for a PMMA % wt. of 40%. This result is displayed quantitatively in Fig. 7, which presents the latent heats of melting and phase transition as functions of PMMA contents.

The melting latent heat decreases continuously until the system becomes amorphous. However, for the phase transitions, the system has two extreme possibilities above 15% of PMMA contents, depending on the sample thermal history (frozen or quasi-equilibrium). Annealing at 90°C, one allows the system to recrystallize, increasing the latent heat of the ferroelectric transition (Fig. 7, open triangles). This can also be done by changing the cooling rates (Fig. 4). It is believed that a higher viscosity, due to the presence of the PMMA amorphous chains, accounts for this kinetic dependence, making difficult the crystallization on cooling.

Storing the samples with more than 15% wt. of PMMA at room temperature for one week or more shifts the ferroelectric phase transition to lower temperatures (Figs. 3 and 5). This phenomenon can be attributed to the crystallization of the anchored amorphous phase [15,16] (a semi-crystalline region on the crystallites surface, which contains several defects). It produces less perfect crystallites with lower ferroelectric transition temperatures. It should be noted that this crystallization process does not change the melting temperatures. We believe that this indicates the presence of "gauche" conformation in the recrystallized material, which constitutes an unstable defect into the "trans" conformation of the ferroelectric phase, but which is characteristic of the helicoidal paraelectric chains [18].

In Fig. 8 we summarize the behavior of the glass, ferroelectric and melting phase transition temperatures with the amount of PMMA in the blends. Additionally, we plot besides the glass transition data, the classical Gordon–Taylor curve for T_g in compatible polymer blends [6]:

$$T_g = \frac{c_2 T_{g2} + c_1 k T_{g1}}{c_2 + c_1 k}, \qquad (1)$$

with $T_{g1} > T_{g2}$. In the above expression, T_g is the intermediate temperature for the blend, T_{g12} the glass transition temperatures for the constituents (see Table 1), $c_{1,2}$ their weight fractions and k is a parameter linked to the ratio between the specific thermal expansion coefficient variations of the two components at their glassy transitions [6]. We note that the theoretical expression describes very well the behavior of the glass transition up to 15% wt. of PMMA but, above this value, only the sample with 30% wt. PMMA showed a glass temperature compatible with this model.
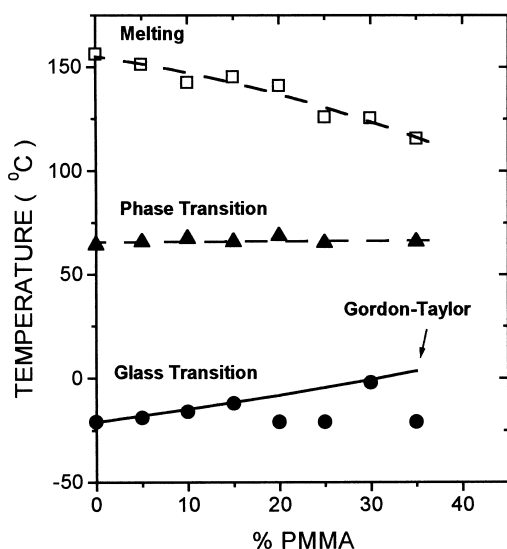

Fig. 8. Melting (open square) and ferroelectric transition (solid triangle) for second heating. The glass transition (solid circles) temperatures for P(VDF–TrFE50%)/PMMA blends are from one week stored samples. The Gordon–Taylor theoretical curve for T_g in polymer blends is also shown (solid line).

Table 1
Molecular weight, specific weight, molar volume, glass transition temperature and melting enthalpy for PMMA and P(VDF–TrFE50%), estimated for a 100% crystalline material [19]

	PMMA	P(VDF–TrFE50%)
MW (g/mol)	100	73.0
ρ(g/cm^3)	1.20	1.88
V_μ (cm^3/mol)	83.3	38.8
T_g (K)	368	251

In order to have a better understanding about the compatibility of the constituents in the blend, let us focus our attention on the melting behavior of the system. The depression of the melting temperatures in the blends could be an indication of the attractive interaction between the polymer chains in the melt. The data of Fig. 8 allow us to determine the interaction parameter χ_{12}, using the model developed in the references [5] and [6]. According to those authors, the melting temperature of a mixture of a crystalline and an amorphous polymer is given by

$$\frac{1}{T_m} = -\frac{V_{2\mu} B \nu_1^2}{\Delta H_m^0 T_m} + \frac{1}{T_m^0},$$ (2)

where T_m^0 is the melting point of the pure crystalline polymer (in our case, the copolymer), T_m is the melting point in the blend, ΔH_m^0 its melting enthalpy for 100% crystallinity, ν_1 the volume fraction of the amorphous component (PMMA in our case) in the blend and V_2 the molar volume of the copolymer. The parameter B allows the determination of the interaction parameter by

$$\chi_{12} = \frac{B V_{1\mu}}{RT}$$ (3)

where $V_{1\mu}$ is the molar fraction of PMMA and R the 'Boltzman constant' (8.31 J/mol.K).

Fig. 9 presents the plot of $1/T_m$ versus ν_1^2/T_m for our data (ν_1 is obtained using the densities given in Table 1). The linear variation shows the validity of the expression (Eq. 2)
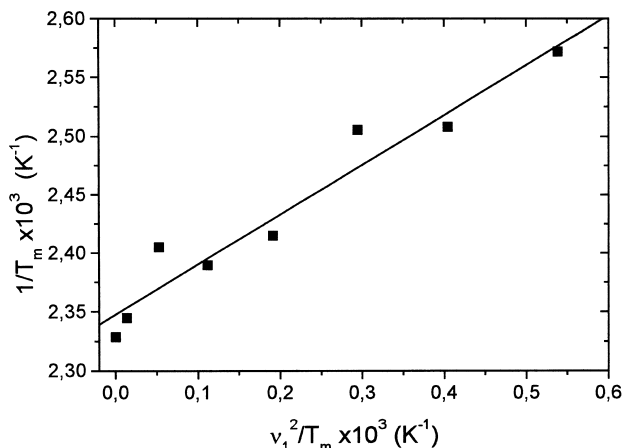

Fig. 9. Plot of $1/T_m$ versus ν_1^2/T_m for P(VDF–TrFE50%)/PMMA blends.

and the positive slope of the straight line indicates that B and χ_{12} are negative, and so, that the different chains attract mutually in the melt. Using the data presented in Table 1 we obtained $B = -(8.5 \pm 0.8)$ cal/cm^3 and $\chi_{12} = -(0.83 \pm 0.08)$ at 156°C.

Although B and χ_{12} were negative and relatively high, indicating a good compatibility in the melt, this is not a sufficient condition for a complete mixing of the constituents at room temperature. In fact, in the range where the crystallization can take place, the increasing glass transition temperature of the mixture, beside the decreasing of crystallization temperature (Fig. 1(b)), lead to the observed metastable behavior of the glassy transitions for increasing PMMA contents.

The evolution of the glass transition temperature confirms that P(VDF–TrFE$_{50\%}$) copolymer and PMMA form stable and fully compatible ferroelectric blends until 15% wt. of PMMA contents. Above this value, until 35%, the formation of blends is still possible, however phase separation in both amorphous and crystalline regions becomes more probable. For this reason, we have observed the strong thermal history dependence of the glassy and ferroelectric behaviors of the blends in this composition range. Above 35%, the system is amorphous but, as reported by Nishi and Wang [5] for PVDF/PMMA blends, if these samples are stored for a while at temperatures below T_c, the P(VDF–TrFE) chains can migrate through the blend and crystallize.

The optical transmission UV–VISA measurements also indicate 15% wt. of PMMA as the limit for improving the transmission efficiency (Fig. 6). The less perfect crystallites, produced at the room temperature by recrystallization of the anchored amorphous phase, also seems to be a feasible explanation for the changing in the optical scattering pattern above this value.

Finally, if we look to high optical transmission efficiency in the visible range and mainly to stable and high content ferroelectric phase, we may suggest the 15% wt. of PMMA as the optimum material content for nonlinear optical applications. For LASER heating thermoluminescence dosimetry purposes, the operative criteria are melting point higher than 140°C [3] and good optical transmission efficiency in the visible range. This leads us to suggest again the 15% wt. of PMMA as the optimum content host material.

5. Conclusion

We have demonstrated the miscibility of P(VDF–TrFE50%) copolymers with PMMA in the melt, until 15% wt. of PMMA contents. In the range of composition between 20% and 35% wt., these two polymers can still form blends but phase separation is more probable. The system is completely amorphous when the PMMA content is higher than 40%. Optical transmission efficiency and kinetic transition studies have credited to the crystallization of the anchored amorphous phase the production of less perfect

crystallites with lower ferroelectric transition temperatures. The kinetic studies also suggest that the strong thermal dependence of the samples with PMMA contents in the range of 20% to 35% wt., is due to both a higher viscosity, which decreases the chain mobility, and the lower crystallization temperatures. Based on the melting and ferroelectric behavior and on the optical transparency analysis, we have found the optimum composition for nonlinear optical and thermoluminescence applications.

Acknowledgements

References

[1] Bürgel A, Kleemann W, Biebricher M, Franke H. Applied Physics 1995;A60:475.

[2] Tsutsumi N, Ono T, Kiyotsukuri T. Macromolecules 1993;26:5447.

[3] Zangaro RA, Gasiot J, Moreau Y. Rad Prot Dosimetry 1990;30(2):111.

[4] Noland JS, Hsu NNC, Saxon R, Schmitt JM. Adv Chem Sci 1971;99:15.

[5] Nishi T, Wang TT. Macromolecules 1975;8(6):909.

[6] Roerdink E, Challa G. Polymer 1978;19:173.

[7] Lovinger AJ. In: Basset DC, editor. Developments in crystalline polymers, vol. 1, chapter 5. London: Applied Science, 1982.

[8] Leonard C, Halary JL, Monnerie L, Broussoux D, Servet B, Micheron F. Polym Comm 1983;24:110.

[9] Domenici C, DeRossi D, Nannini A, Verni R. Ferroelectrics 1984;60:61.

[10] Hahn BR, Herrmann-Schönherr O, Wendorff JH. Polymer 1987;28:201.

[11] Furukawa T, Date M, Fukada E, Tajitsu Y, Chiba A. Jpn J Appl Phys 1980;19(2):L109.

[12] Tajitsu Y, Chiba A, Furukawa T, Date M, Fukada E. Appl Phys Lett 1980;36(4):286.

[13] Lovinger AJ, Davis GT, Furukawa T, Broadhurst MG. Macromolecules 1982;15:323.

[14] Lovinger AJ. Science 1983;220(4602):1115.

[15] Moreira RL, Saint-Gregoire P, Lopez M, Latour M. J Polymer Sci: Polym Phys Ed 1989;27:709.

[16] Moreira RL, Almairac R, Latour M. J Phys: Condens Matter 1989;1:4273.

[17] Scherrer P. Nachr Göttinger Gessel. 98, 1918.

[18] Tashiro K, Kobayashi M. Polymer 1988;29:426.

[19] Moreira RL, Lobo RPSM, Medeiros-Ribeiro G, Rodrigues WN. J Polym Sci: Polym Phys 1994;32:953.

[20] Lovinger AJ, Davis GT, Furukawa T, Broadhurst MG. Macromolecules 1982;15:329.